

UNCLASSIFIED

AD NUMBER

AD822944

LIMITATION CHANGES

TO:

Approved for public release; distribution is unlimited.

FROM:

Distribution authorized to U.S. Gov't. agencies and their contractors; Critical Technology; NOV 1967. Other requests shall be referred to Army Electronics Command, AMSEL-KL-SM, Fort Monmouth, NJ. This document contains export-controlled technical data.

AUTHORITY

usaec ltr, 30 jul 1971

THIS PAGE IS UNCLASSIFIED

AD

RESEARCH AND DEVELOPMENT TECHNICAL REPORT
ECOM-01758-7

GUNN EFFECT DEVICES

SEVENTH QUARTERLY TECHNICAL REPORT

By

J. BARRERA

NOVEMBER 1967

ECOM

UNITED STATES ARMY ELECTRONICS COMMAND • FORT MONMOUTH, N.J.

CONTRACT DA 28-043 AMC-01758(E) - ARPA Order No. 692
HEWLETT-PACKARD COMPANY
HEWLETT-PACKARD LABORATORIES
Palo Alto, California

The work prepared under this contract is a part of PROJECT DEFENDER and was made possible by the support of the Advanced Research Projects Agency under Order No. 692, through the U. S. Army Electronics Command.

DISTRIBUTION STATEMENT

This document is subject to special export controls and each transmittal to foreign governments or foreign nationals may be made only with prior approval of Commanding General, U. S. Army Electronics Command, Fort Monmouth, New Jersey.
Attn: AMSEL-KL-SM

NOTICES

Disclaimers

The findings in this report are not to be construed as an official Department of the Army position, unless so designated by other authorized documents.

The citation of trade names and names of manufacturers in this report is not to be construed as official Government indorsement or approval of commercial products or services referenced herein.

Disposition

Destroy this report when it is no longer needed. Do not return it to the originator.

Research and Development
Technical Report ECOM-01758-7

NOVEMBER 1967

GUNN EFFECT DEVICES

SEVENTH QUARTERLY TECHNICAL REPORT
15 June 1967 to 15 September 1967

Report No. 7

Contract No. DA 28-043 AMC-01758(E)
ARPA Order No. 692
O/S Task No. 7900.21.243.38.00

Prepared by

J. Barrera

HEWLETT-PACKARD COMPANY
Hewlett-Packard Laboratories
Palo Alto, California

for

U. S. Army Electronics Command, Fort Monmouth, New Jersey

The work prepared under this contract is part of PROJECT DEFENDER and was made possible by the support of the Advanced Research Projects Agency under Order No. 692, through the U. S. Army Electronics Command.

DISTRIBUTION STATEMENT

This document is subject to special export controls and each transmittal to foreign governments or foreign nationals may be made only with prior approval of the Commanding General, U. S. Army Electronics Command, Fort Monmouth, New Jersey.
Attn: AMSEL-KL-SM

ABSTRACT

A shift from emphasis on device technology to device parameter variation and performance has been made. To date, over 60 MW of CW power has been obtained at 3.5 GHz but with poorer noise behavior than has been reported for lower power devices. Over 1000 hours of CW operation has been achieved for a few TE 144 samples with no measurable deterioration of D. C. or RF behavior.

Considerable effort has been made to correlate known material doping gradients to poor RF behavior and lack of current drop at threshold. Two simple FM noise measurement systems are described and further computer results for LSA mode operation are presented.

PURPOSE

A development program is to be conducted aimed at the utilization of the Gunn effect for various types of microwave generating devices in the 1 to 50 GHz frequency range. Spectral line width should be less than 10kHz and operation should be in a single mode. Output power should be at least 25 mW in CW operation and 3W peak in pulsed operation with a conversion efficiency of at least 3%. CW operation should be obtained in ambient temperatures from -25°C to +50°C with a single device.

Application of these devices for amplification and modulation is to be investigated.

FOREWORD

The work reported on in this report has been authorized by the Contracting Officer, Mr. Edgar D. Fitzgerald, Electronic Components Laboratory, U. S. Army Electronics Command, Ft. Monmouth, New Jersey, under Contract No. DA 28-043 AMC-01758(E) and titled "Gunn Effect Devices". The Project Engineer at the U. S. Army Electronics Command is Mr. Maurice Druesne.

The work has been performed at Hewlett-Packard Laboratories under the supervision of M. M. Atalla. The report has been prepared by J. Barrera. Significant contributions during the report period have been made by N. Mantena, G. W. Mathers, E. Gowen, B. Farrell and T. Fortier. Discussions with M. M. Atalla and C. F. Quate were of great benefit.

TABLE OF CONTENTS

<u>Section</u>	<u>Title</u>	<u>Page</u>
I.	Device Fabrication and Measurement	1
I. 1	Introduction	1
I. 2	Performance Summary	3
I. 3	Doping Profile Evaluation	10
I. 4	Life Testing	14
I. 5	Contact Resistance	14
I. 6	Discussion	16
II.	Noise Measurements	20
II. 1	Device and Measurements	20
II. 2	FM Noise System	20
III.	Computer Studies	26
III. 1	LSA Mode Simulation	26
IV.	Conclusions	32

I. DEVICE FABRICATION AND MEASUREMENT

I. 1 Introduction

During all the preceding quarters a clear emphasis has been placed on work involving device technology. In the very early stages great effort was expended to achieve CW operation of negative temperature coefficient material; to provide ohmic contacts to a large range of material resistivities; and, in general, to obtain a trouble-free die attaching and external contacting procedure. To date a technology has been developed which does accomplish the above tasks successfully. With the advent of HPL solution grown GaAs, the technology was advanced further and confidence in device fabrication achieved to the extent that emphasis could be shifted to optimization of device performance. The work of the later quarters and the present quarter has, then, dealt primarily with the study of device performance with regard to RF power, FM noise and general characteristic stability. The above performance indices have been observed with respect to device geometry, microwave circuitry, and, most importantly, to actual GaAs material parameters.

Work during the present quarter has specifically involved evaluation of doping profiles in the GaAs used for devices and the possible correlation of such profiles with the general microwave performance. It is suspected that gradients in doping are responsible for asymmetry in the high field I-V characteristic and for the very small current drops observed at threshold.

Further testing of TE 113 devices will be reported along with results of less extensive testing of several other groups of devices-- among which are TE 144's, TE 158's and TE 166s.

It is believed that the LSA mode of operation has been observed but due to a too low nl product and n/f ratio for the TE 113 devices involved, the RF power out was not exceptional.

Various diagnostic experiments have been performed and will be briefly noted in the following sections. Included are the results of a life test on a TE 144 sample, the contact resistance evaluation of the standard 4-layer contact used on HPL Gunn effect devices, and an example of doping gradient measurements on a poor run of solution grown GaAs.

I. 2 Performance Summary

Another group of devices, designated TE 144's, have been processed from HPL solution grown GaAs material and fairly extensive RF tests have been made on a number of these devices. A summary of the TE 144 characteristics is given in Table I, where, for comparison a tabulation has been made of corresponding data for TE 65 and TE 113 samples previously tested.

It should be noted that these TE 144 devices had quite a large variation in threshold current and low field resistance. It is suspected that this was due to an accidental overheating during processing which in the past has also led to low field resistance variation in other devices.

The FM noise behavior of the TE 144 devices is considerably poorer than for the TE 113 especially at frequencies close to the carrier (see noise section below).

Several of the TE 113 and TE 144 samples have been tested in the new 6-12 Ghz ridge guide cavity for tunability and maximum available power output. Nearly all the samples have behaved similarly with typical results being shown in Figs. 1 and 2. The relatively low efficiency and low current drop above threshold is believed associated with a doping profile in the material that produces an equivalent positive resistance in series with the device. The power drop off at high frequencies is suspected partially due to this and to the loading of the excess

TABLE I

Device Designation	TE 65	TE 113	TE 144
No. of Samples Tested	25	37	9
Resistivity (Ω cm)	0.9	1.5	2.5
Temp. Coeff. of Resistance	(+)	(+)	(+)
Thickness (microns)	20-25	14-20	14-17
Contact Dot Diam. (microns)	75	105	125
Threshold Voltage (volts)	6.5 - 8.5	5.0 - 6.5	6.0 - 7.0
Threshold Current (ma)	70-90	90-130	80-200
Operating Frequency (GHz)	(1) 8.7 - 8.9 (2) 6.2 - 6.3	8.0 - 8.4 6.1 - 6.2	8.3 - 8.5 6.0 - 6.2
RMS Freq. Deviation in 1 KHz Bandwidth, 10 KHz from the carrier (sec ⁻¹) (voltage range)	300 @ 8.7 GHz (8 - 10 v) 120 @ 6.2 GHz (10 - 12 v)	50 @ 8.3 GHz (10 - 16 v) 24 @ 6.15 GHz (16 - 20 v)	170 @ 8.4 GHz (10 - 11 v) 300 @ 6.1 GHz (10 - 20 v)

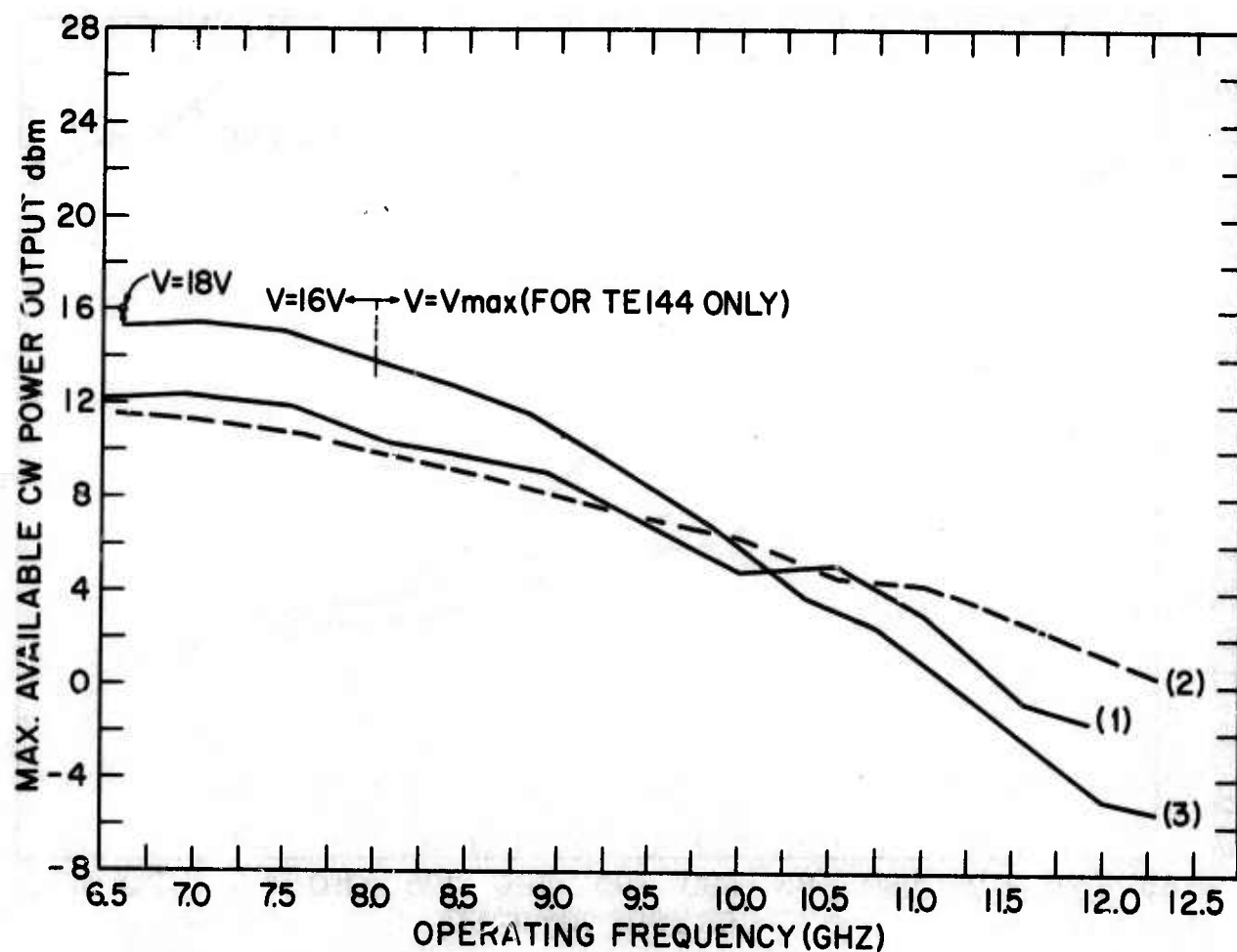


FIG. 1: Maximum Available Power Output

For -- (1) TE 113 #23A, $I_{dc} = 130 - 134$ ma
 (2) TE 113 #34A, $I_{dc} = 100 - 104$ ma
 (3) TE 144 #6, $I_{dc} = 83 - 100$ ma

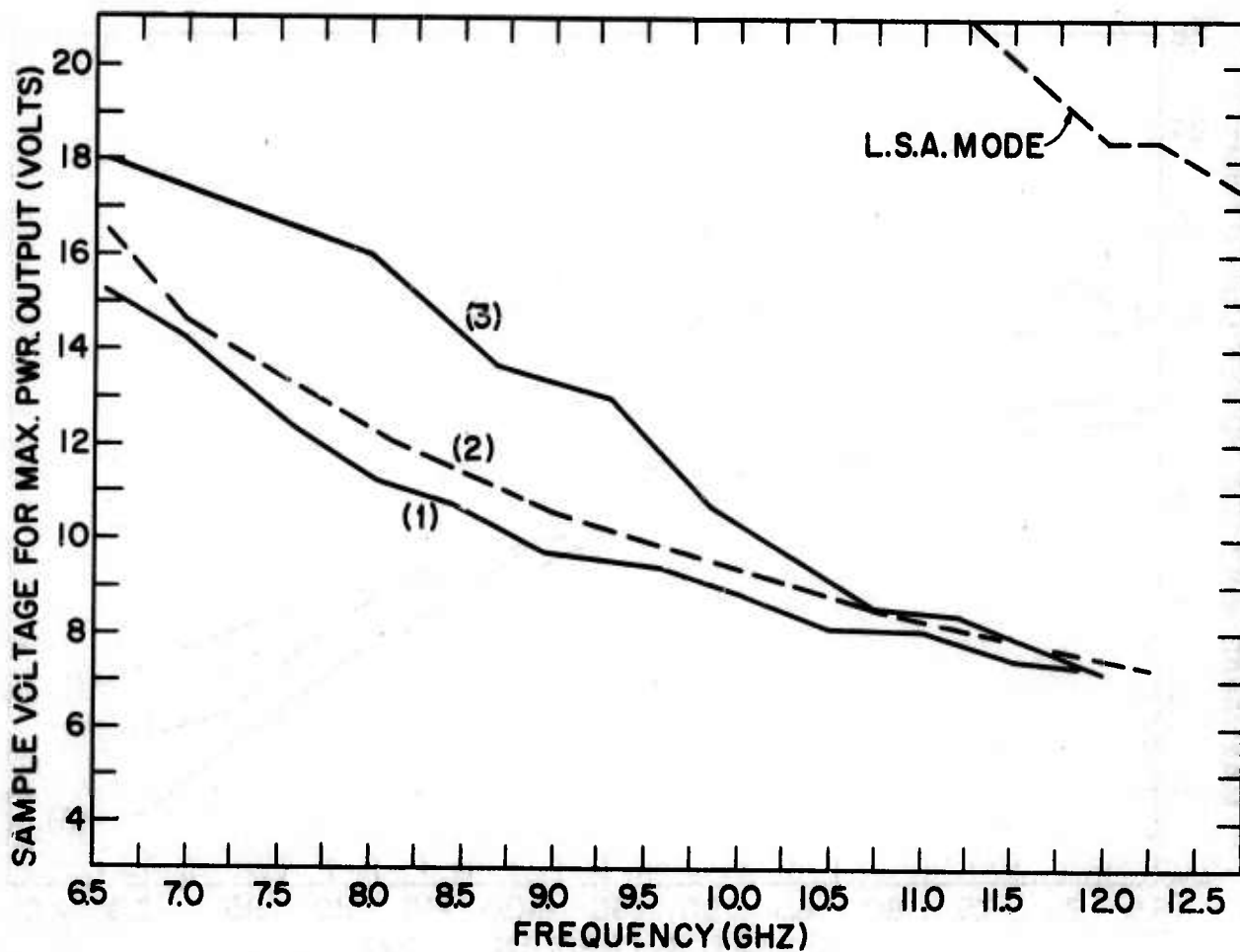


FIG. 2: Voltage Tuning Curve at Maximum Power Output

For -- (1) TE 113 #23A, $V_{TH} = 5.6V$

(2) TE 113 #34A, $V_{TH} = 5.7V$

(3) TE 144 #6, $V_{TH} = 7.0V$

material around the active region of the device. Both of these effects are being studied in more detail but no definite conclusions have been reached as yet.

Rather interesting behavior has been observed with most of the TE 113 and TE 144 devices when operated in the ridge guide cavity (described previously) and also in a new X-band waveguide cavity. With reference to Fig. 3. the frequency and power output of a device are shown as a function of the applied voltage. In this case the cavity tuning is fixed to give an operating frequency of about 11 GHz at a voltage slightly above threshold. As the sample voltage is increased the frequency starts to decrease slowly then quite rapidly to about 8.0 GHz while the power (in this case for light loading) decreases very rapidly to near zero output. In the range of voltages where the rapid frequency decrease is observed, the cavity tuning has very little control of the frequency. At a certain voltage (≈ 15 to 18 volts) the frequency suddenly jumps back to a somewhat higher value than it had originally, this frequency being almost independent of voltage but again controllable by the cavity tuning.

The maximum available power output and the FM noise for this high voltage-high frequency operation is nearly the same, for the same frequency, as is obtained at lower voltage operation (see Figs. 1 and 2). The upper frequency limit for this high voltage operation is between 12 and 13 GHz; the limit being mechanical tuning of the cavity.

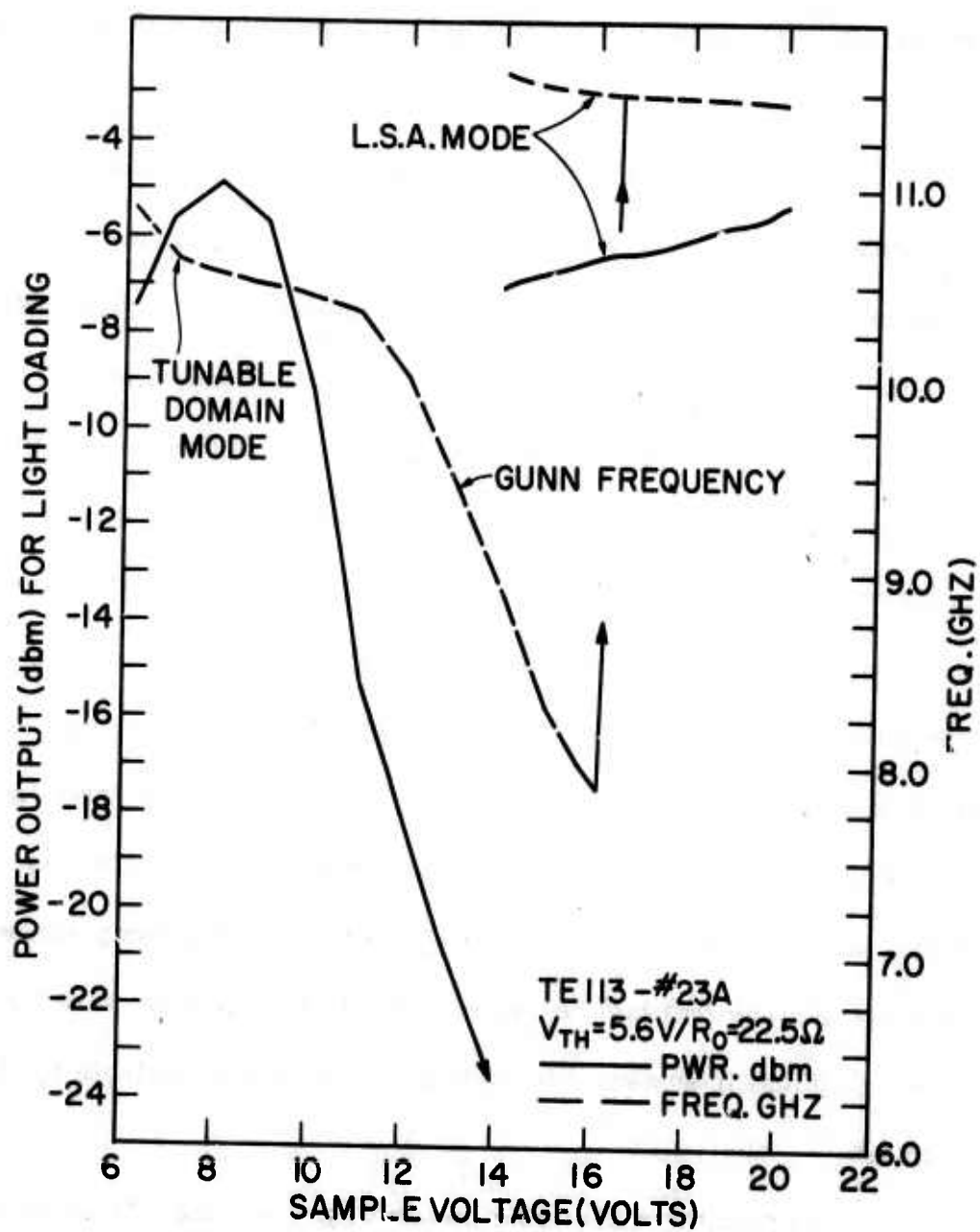


FIG. 3: Voltage Tuning Curve for Light Loading And Fixed Cavity Tuning

The lower frequency limit is between 9 and 10 GHz; this limitation being determined by the maximum allowable voltage (power dissipation) for the device. As the cavity tuning is adjusted to lower the frequency, the device voltage has to be increased in order to keep operating in the same mode otherwise the frequency will switch back to between 6.5 and 8.0 GHz.

The high voltage mode is, in all probability, the LSA mode of operation but further experimental work with new samples is required to establish this more firmly. The "LSA" mode characteristics were not exceptional, especially regarding RF power, perhaps because the device parameters were outside the ranges established by other workers for the true LSA mode. The nl product for the TE 113 device was approximately $8 \times 10^{11} \text{ cm}^{-2}$.

Preliminary results of tests on new TE 166 devices have shown that although a doping gradient was present in the material used, there is still a fair amount of RF power developed. The samples that have been tested show consistently a CW output of over 60 mw at about 3.5 GHz. The efficiency is typically only 1% and the noise behavior is poor. The low efficiency, poor noise behavior and small threshold current drop are, again, tentatively ascribed to the doping gradient in the starting material.

It is noted that with the present technology, all the new devices are capable of handling around 5 to 7 watts of input power (CW) for a power to total device volume ratio of over 10^6 w/cm^3 .

I. 3 Doping Profile Evaluation

Several runs of HPL solution grown GaAs were suspect because of different growth conditions brought on by a move to a new laboratory area. Because of these unavoidable changes (new gas lines, temperature controllers, etc.) the initial growths were monitored very carefully especially with regard to material homogeneity. In due course it was decided to evaluate all the runs of GaAs, with respect to doping profile in particular, and to correlate device performance with the amount of measured resistivity gradient.

The technique used is a common one. Schottky barriers are made from the same material to be used for devices and the capacitance as a function of reverse bias voltage is measured. The space charge capacitance is quite generally given as

$$C = \frac{\epsilon A}{W}$$

where ϵ is the absolute dielectric constant of the material, A the area and W the depletion depth. Now, if one evaluates the derivative of $1/C^2$ with respect to reverse bias voltage, V , there obtains,

$$\frac{d(1/C^2)}{dV} = \frac{-2}{C^3} \frac{dC}{dV} = \frac{2W}{\epsilon^2 A^2} \frac{dW}{dV}$$

By allowing a small displacement of depletion depth (accomplished practically by a small A. C. voltage swing superimposed on the D. C. reverse bias) and invoking Gauss' law it is easily shown that,

$$\frac{dW}{dV} = \frac{\epsilon}{q N_{(W)} W}$$

where $N_{(W)}$ is the number giving net doping, $N_D - N_A$, at that point where W is the depletion region depth. Thus, the net space charge profile is given by,

$$(N_D - N_A)_{(W)} = \frac{2}{\epsilon q A^2} \cdot \left(\frac{1}{\frac{d(1/C^2)}{dV}} \right)$$

In practice a bridge set up is used to measure C vs. V and a computer routine utilized to give a plot of $N_D - N_A$ as a function of distance in the material.

Figure 4 shows such a plot for TE 158 material. The devices made from this material used the first 30 microns as shown and consequently had a gradient in total doping of 2 to 1. As expected, the performance of the TE 158 devices was quite poor. For example, the IV characteristic showed no current drop at the onset of oscillation and a gross asymmetry when the bias polarity was reversed - see Figure 5.

Although the TE 158 material was an exceptionally poor run the results so far do seem to correlate insignificant device performance with a known resistivity gradient. More work will be done on establishing this trend.

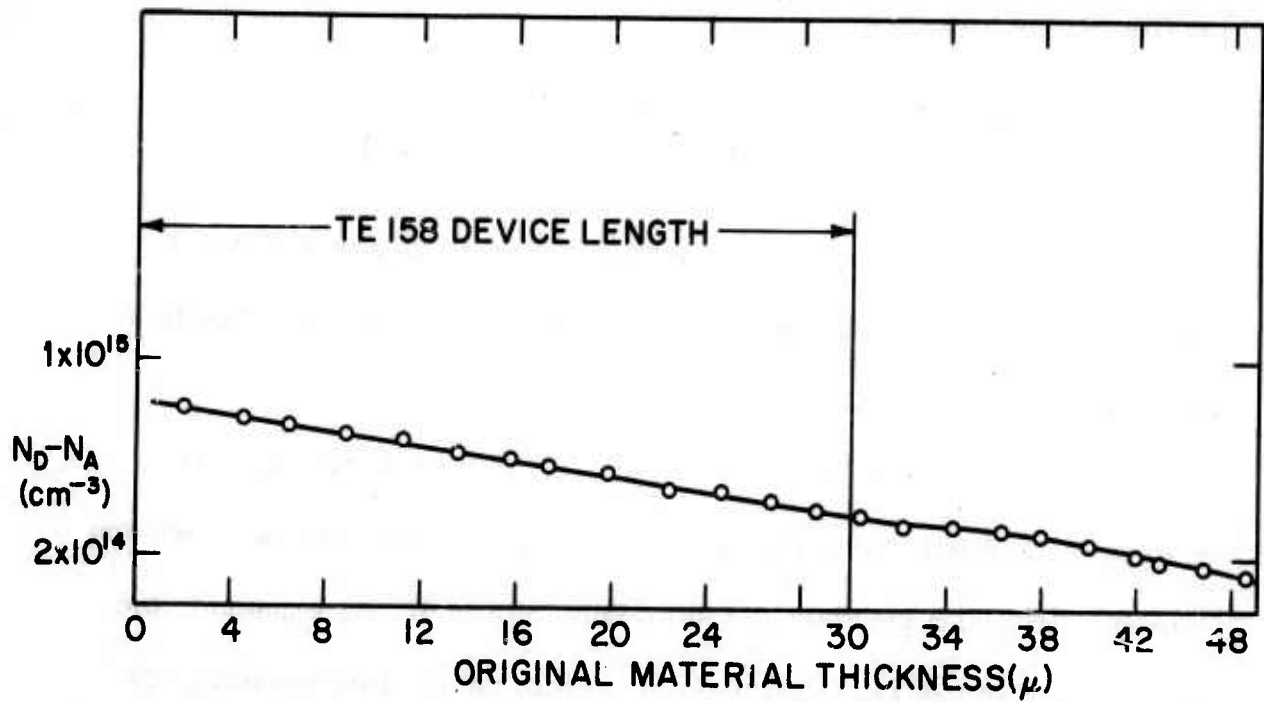


FIG. 4: Total Doping Profile for TE 158 Device Material

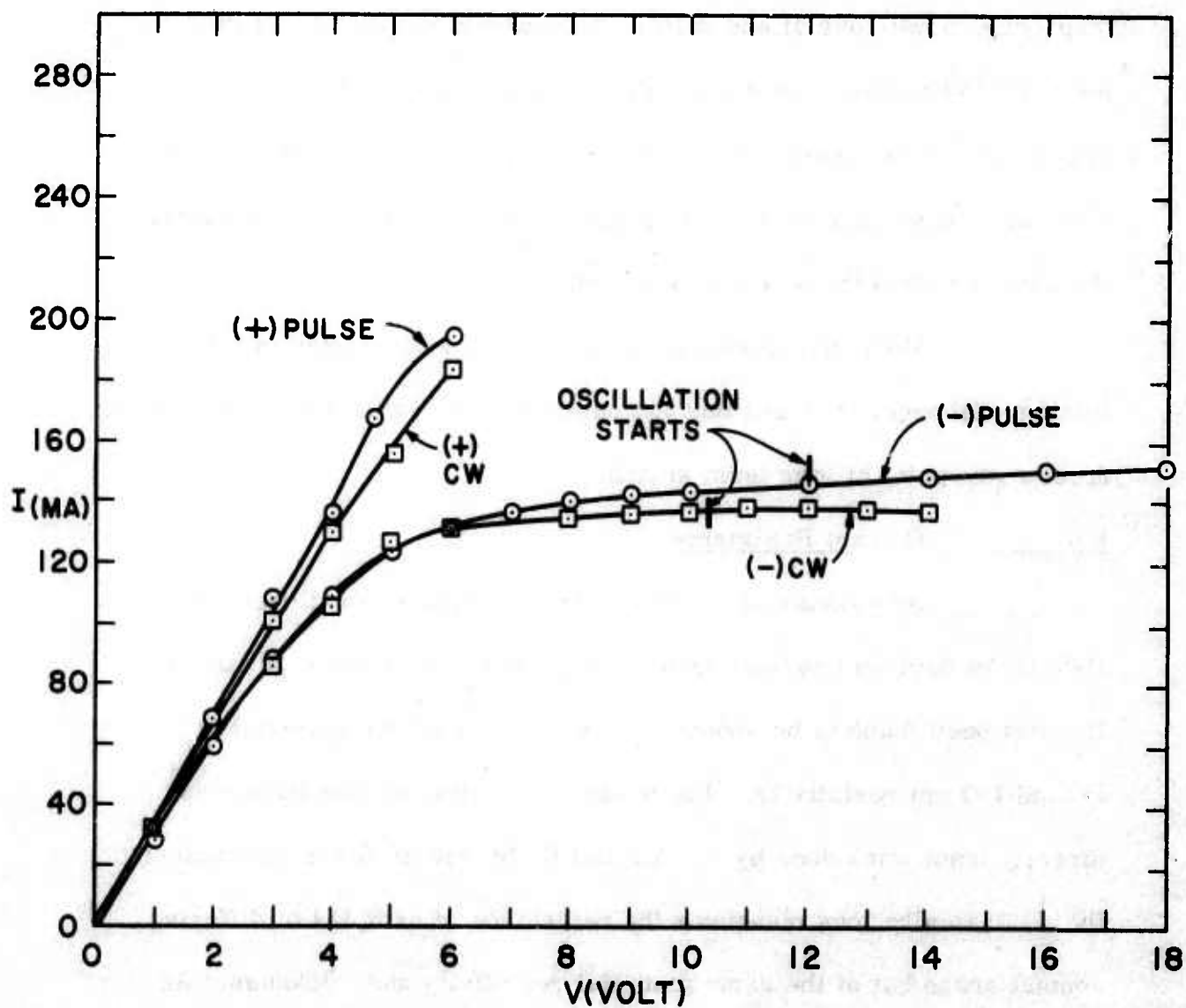


FIG. 5: Typical IV Plot For TE 158 Devices

I. 4 Life Testing

Although a "standard" device has not yet been evolved it was decided to check out the stability of a few devices with respect to frequency, power output and noise. An example is given in Table 2 for a TE 144 device. As shown, the characteristics of the device effectively did not change with over 1000 hours of running time. The test was stopped and the D. C. characteristics were found to be exactly the same as when the test was initiated.

More stringent input power levels will be used in future testing, although, it is felt that the data shown in Table 2 are encouraging from a viewpoint of long term stability.

I. 5 Contact Resistance

An evaluation of the standard 4-layer contact used for HPL GaAs devices has been made. The contact resistance parameter, R_c , has been found to be about $1 \text{ to } 2 \times 10^{-4} \Omega \text{ cm}^2$ for material of around $1 \Omega \text{ cm}$ resistivity. The method of evaluation was borrowed directly from work done by R. Cox and H. Strack of Texas Instruments, Inc.¹ Basically, one measures the resistance of samples of differing contact areas but of the same material resistivity and thickness. An empirically determined factor $B \left(\frac{d}{t} \right)$ is used to relate the calculated sample spreading resistance to the actual sample bulk resistance and

1. "Ohmic Contacts for GaAs Devices" to be published in Solid State Electronics.

TABLE 2 - LIFE TEST

SAMPLE NO. TE 144-6		$V_{\text{Bias}} = 2 \cdot V_{\text{Threshold}}$	% Eff \approx 1.3%
TIME (Hrs.)	FREQUENCY (GHz)	POWER (MW)	FM NOISE (Hz) @ 10 KHz in 1 KHz BW
0	8.433	13.18	100
96	8.431	12.30	100
144	8.433	12.59	96
436	8.432	12.59	104
720	8.431	12.88	80
1036	8.432	12.30	98

the contact resistance contribution is added directly as a function of contact area. The total sample resistance is then given as

$$R_t = \frac{\rho}{2d} \cdot B \left(\frac{d}{t} \right) + \frac{4 R_c}{\pi d^2} \cdot C$$

where ρ is the resistivity, d the dot diameter, t the thickness and C a multiplier which for the case at hand is about 2 since the n material is not on an n^+ substrate and the back overlay contact resistance is on the order of the dot contact resistance.

The actual dot pattern used is shown in Figure 6 with the largest dot being 7.30 mil in diameter. By knowing the thickness, resistivity and contact diameter of the samples a fit can be made to the measured total resistance curves as a function of $1/2d$. A typical curve fit is shown in Figure 7 for $1.06 \Omega \text{ cm}$ material with a resulting specific contact resistance of $1.5 \times 10^{-4} \Omega \text{ cm}^2$.

The above result is good within an expected error of 15 to 30%. The indication is, however, that the contact is of relatively low resistance and although not evaluated as above, the general contact has proved to provide good ohmic behavior to resistivities from $0.5 \Omega \text{ cm}$ to over $20 \Omega \text{ cm}$.

I. 6 Discussion

The work of the preceding sections is continuing with the goal of producing a low noise, relatively high power CW and pulsed device.

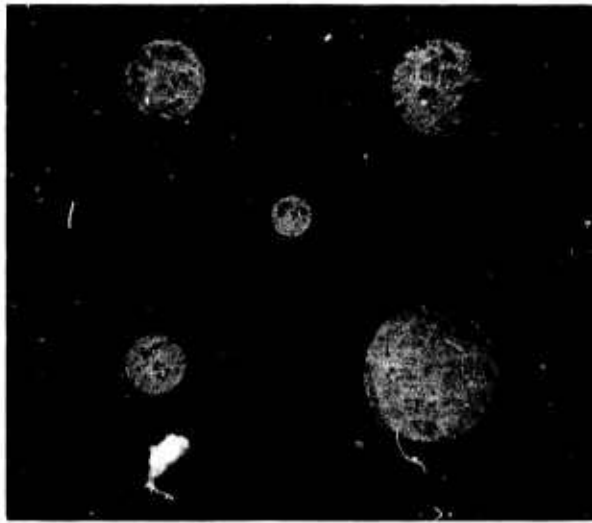


FIG. 6: Dot Pattern For Contact Resistance Experiment

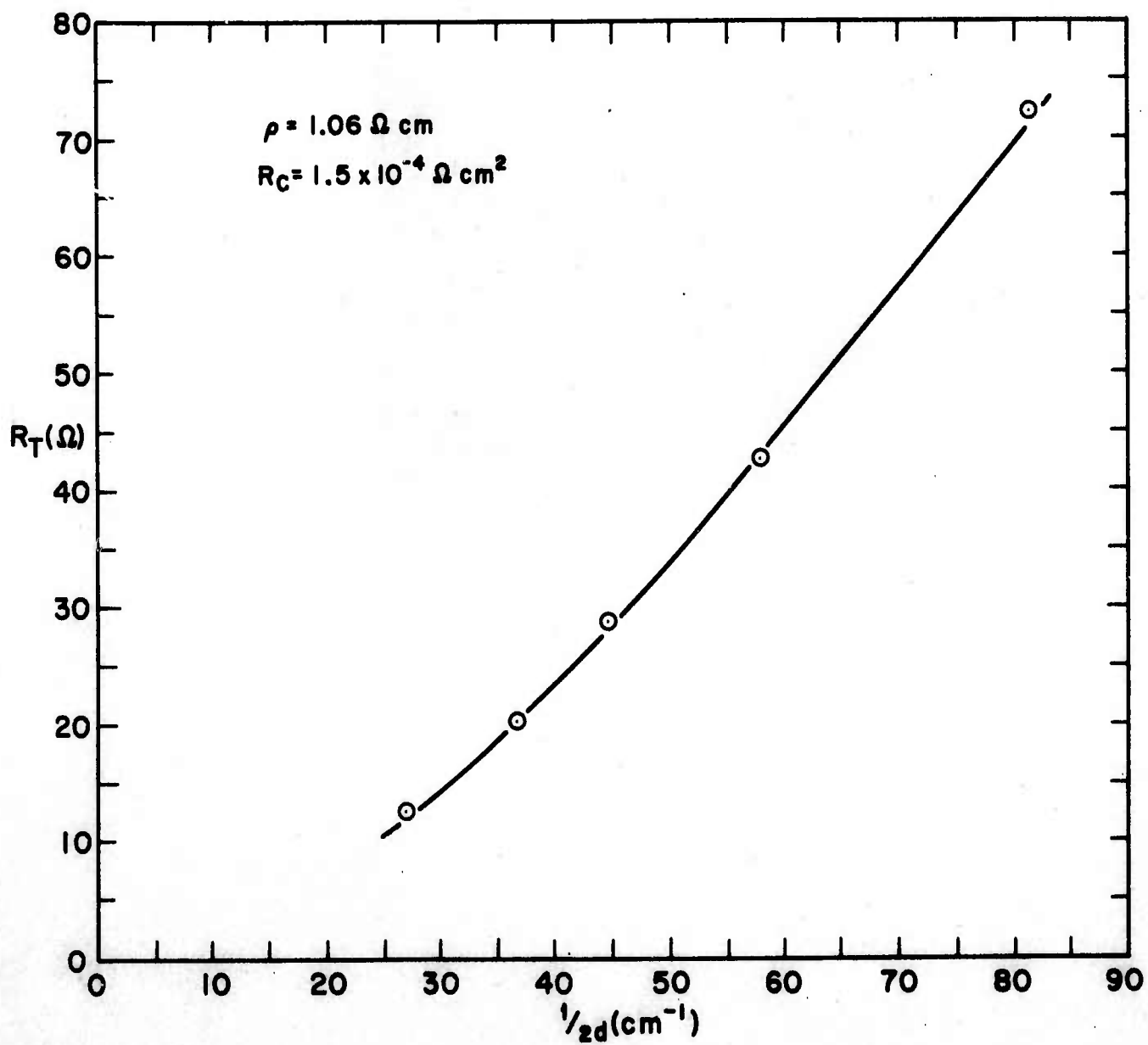


FIG. 7: Total Resistance vs. Inverse Of Twice Dot Diameter

— Calculated
 ○ Measured

Much freedom is being exercised in combining device geometry, material parameters and microwave circuitry to give the desired results.

A good correlation is being sought between RF and high field D. C. behavior and material inhomogeneity and effort is being made to produce material with less than 5% doping gradient by solution grown epitaxy. Endeavor is also being made to utilize all the better points of the present device fabrication and technology to achieve the above mentioned performance goals.

II. NOISE MEASUREMENTS

II. 1 Device and Measurements

Current and FM noise measurements are being taken on a routine basis for all devices under test. In particular, a low field current noise spectrum is taken as an indicator of contact quality. Also, a current noise spectrum around threshold bias is taken along with FM noise spectra at various carrier frequencies in order to check for possible correlation between the two noises.

As mentioned in Section I, the FM noise of TE144 samples was not as low as for TE 113's especially at frequencies very close to the carrier. In Figure 8 a typical FM spectrum of TE 113 and TE 144 samples is shown (along with an older TE 65 and Monsanto sample curve). The spectra tend toward one another at large frequency deviation from the carrier but at lower frequencies the difference is significant.

It is interesting to compare the magnitude of the short circuit noise current around threshold bias with the magnitude of the FM noise. Figure 9 shows the various current noise vs. bias voltage curves for the same samples as used in Figure 8. As has been mentioned previously there is usually a correlation between the magnitudes but a direct relation is not always the case.

II. 2 FM Noise System

The system used to measure the FM noise of HPL GaAs devices is a fairly simple one. In its basic form one can obtain a measure

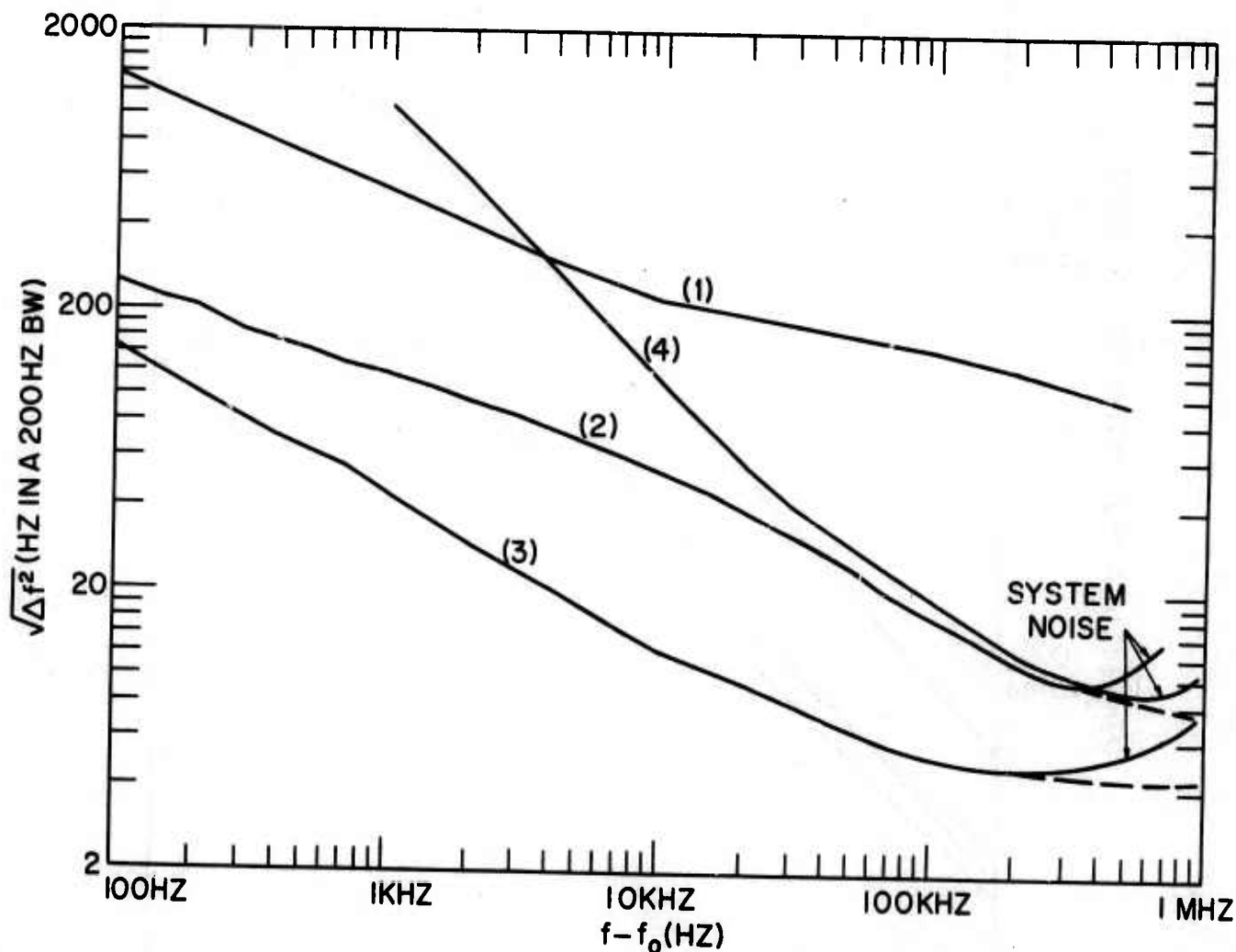


FIG. 8: RMS Frequency Fluctuation Away From The Carrier

- For -- (1) Monsanto Material Device, $f_0 = 4.97$ GHz, $V/I - 8.7$ V/282 ma
 (2) TE 65 #10, $f_0 = 4.96$ GHz, $V/I - 11.0$ V/65 ma
 (3) TE 113 #34A, $f_0 = 6.09$ GHz, $V/I - 17.0$ V/110 ma
 (4) TE 144 #6, $f_0 = 8.28$ GHz, $V/I - 12$ V/84 ma

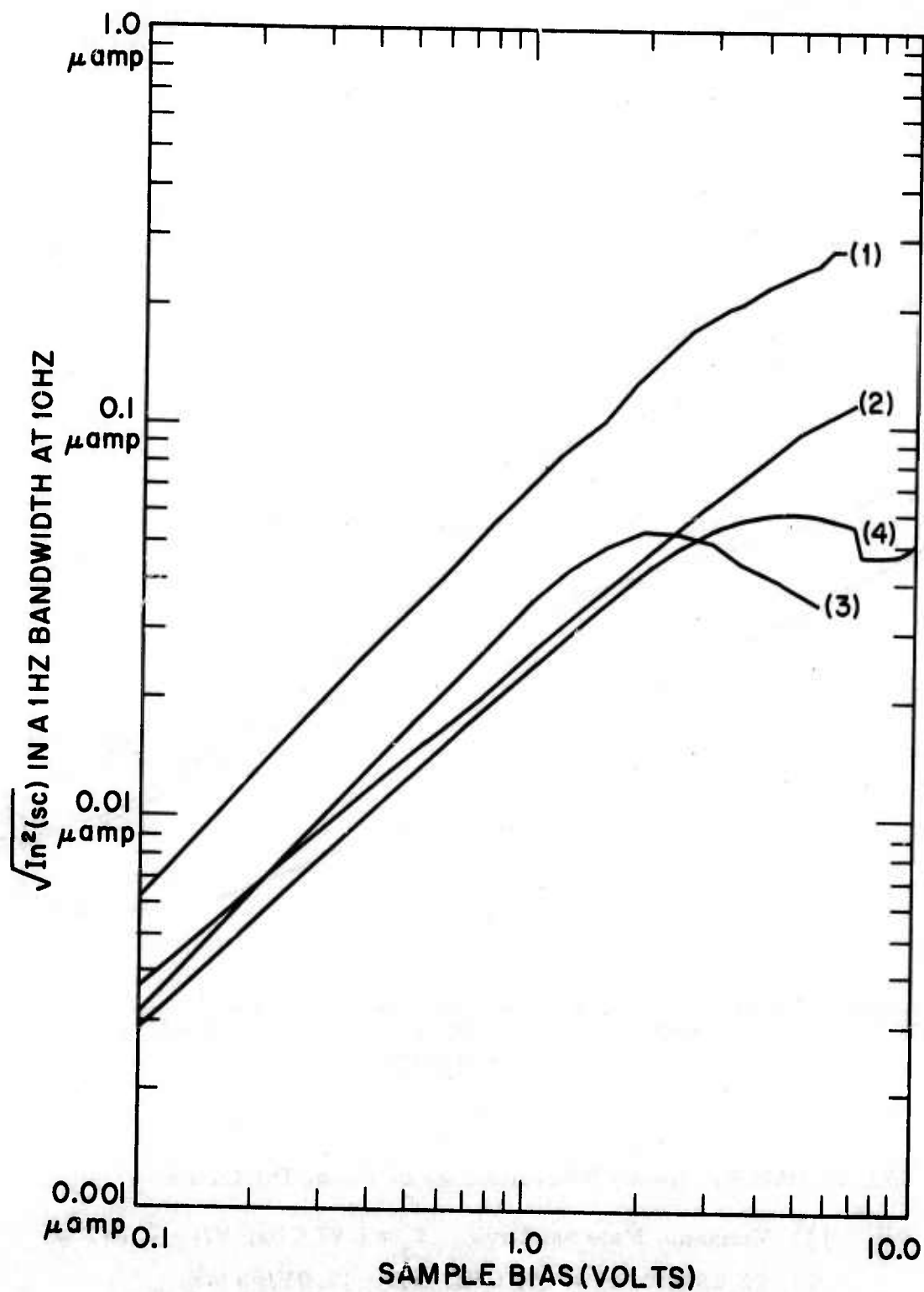


FIG. 9: RMS Short Circuit Noise Current vs. Bias Voltage for Samples Shown in Figure 8 with

$$V_{TH(1)} = 6.5V$$

$$V_{TH(2)} = 7.2V$$

$$V_{TH(3)} = 5.7V$$

$$V_{TH(3)} = 7.0V$$

of frequency fluctuation vs. frequency deviation from a carrier for levels approaching the FM noise levels of good klystrons. The FM noise of the system can be traced back to the quality of the reference oscillator used which, in the first set up to be described, is not a crystal oscillator.

The system used, in functional form, is as shown in Figure 10. A signal from the oscillator under test is coupled out of the cavity directly into an -hp- 2590B Microwave Frequency Converter. The 2590B contains a tunable oscillator (240 MHz to 390 MHz) whose output is used to generate multiply related frequencies which are in turn used to mix with the incoming signal. The nominally 30 MHz IF is then fed into a very linear discriminator whose output is Fourier analyzed using an -hp- 310A Wave Analyzer. By knowing the sensitivity of the discriminator ($5 \mu\text{v}/\text{Hz}$), the RMS amplitude of the output can be translated into RMS frequency fluctuation in a known bandwidth at the desired frequency from the carrier.

The second system shown in Figure 11 is an improvement on the first system in that an external, tunable microwave source, phase locked to a crystal oscillator, is used for fundamental mixing with the incoming microwave signal. The 2590B is then just used as a discriminator. The improved frequency stability of the reference oscillator thus lowers the system FM noise level to a point where a few cycles deviation can be detected.

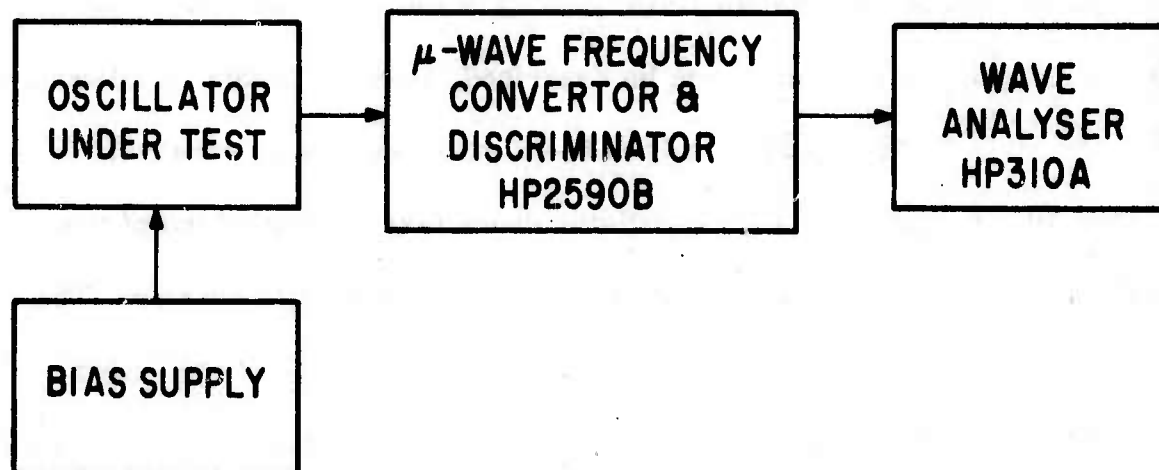


FIG. 10: Schematic Of First FM Noise Measuring System

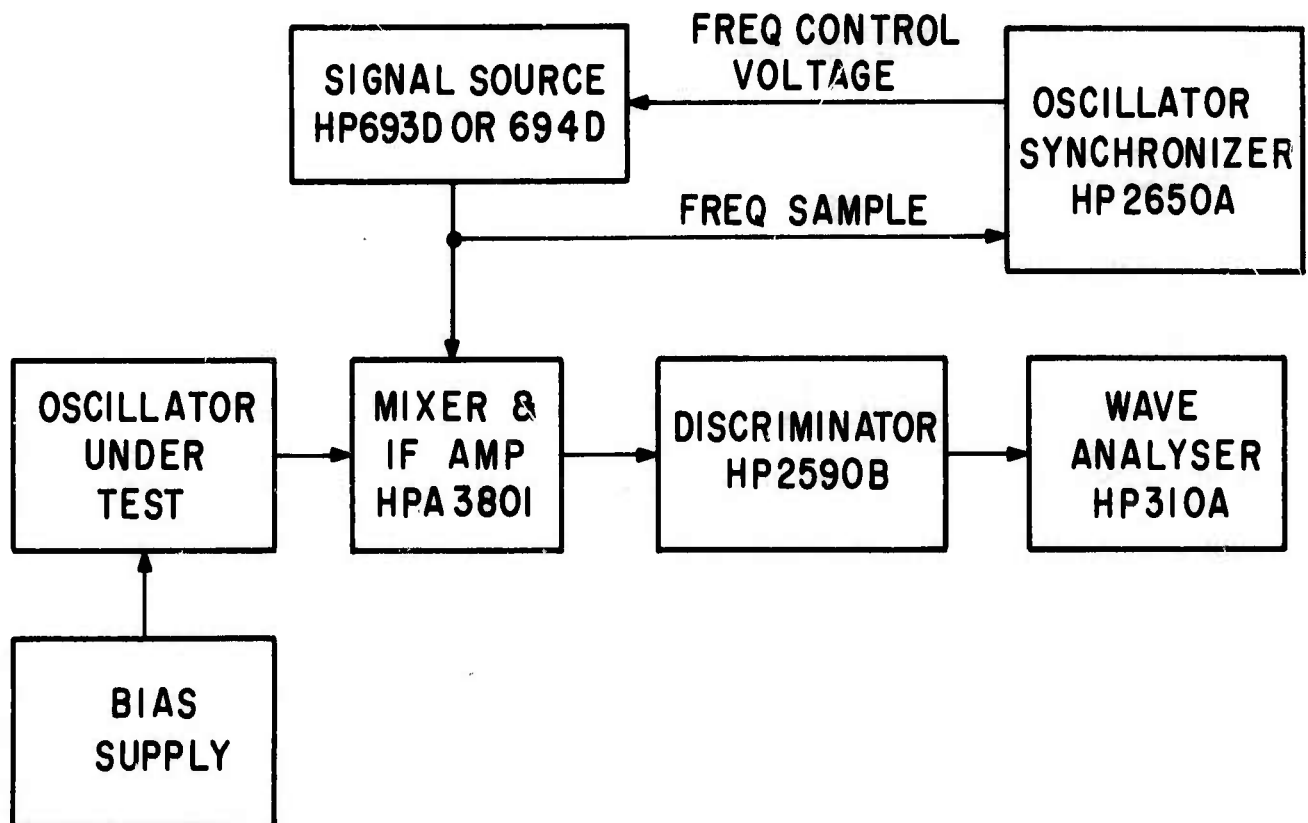


FIG. 11: Schematic Of Second FM Noise Measuring System

III. COMPUTER STUDIES

III. 1 LSA Mode Simulation

Some preliminary results of computer calculations on LSA mode simulation were given in the last quarterly report. During this quarter, more physical insight and design information has been obtained for samples utilizing the LSA mode of operation. For an example of the calculations involved a sample 20 microns in length with 10^{15} carriers per cc with a threshold field of 3.5 KV/cm was used in conjunction with a simple R, L, C circuit resonating at 8.6 GHz and possessing a Q of 100. Plots were produced of sample voltage and current and the integral of differential mobility, V_{st} , I_{st} and $\int \mu_d dt$ respectively, as a function of time. The plots are shown in Figures 12, 13 and 14 for the sample biased at twice $V_{threshold}$ (14 volts). All the quantities show steady state variation after the third RF cycle due to the initial conditions provided. The most significant plot is the $\int \mu_d dt$ variation with time. In the steady state, the net contribution to the integral over an rf period is positive and the value of $\int \mu_d dt$ increases steadily. Although V_{ST} stays above V_{TH} for a major fraction of the rf period, the device stays in the positive resistance region longer than it is necessary to decay any accumulated charge. Thus, the calculations showed a conversion efficiency of only 0.8% with a power output of 15 MW and a d. c. power input of 1.89 watts.

As Q was decreased, the rf loading became more favorable and the slope of the $\int \mu_d dt$ curve between two successive points of the rf

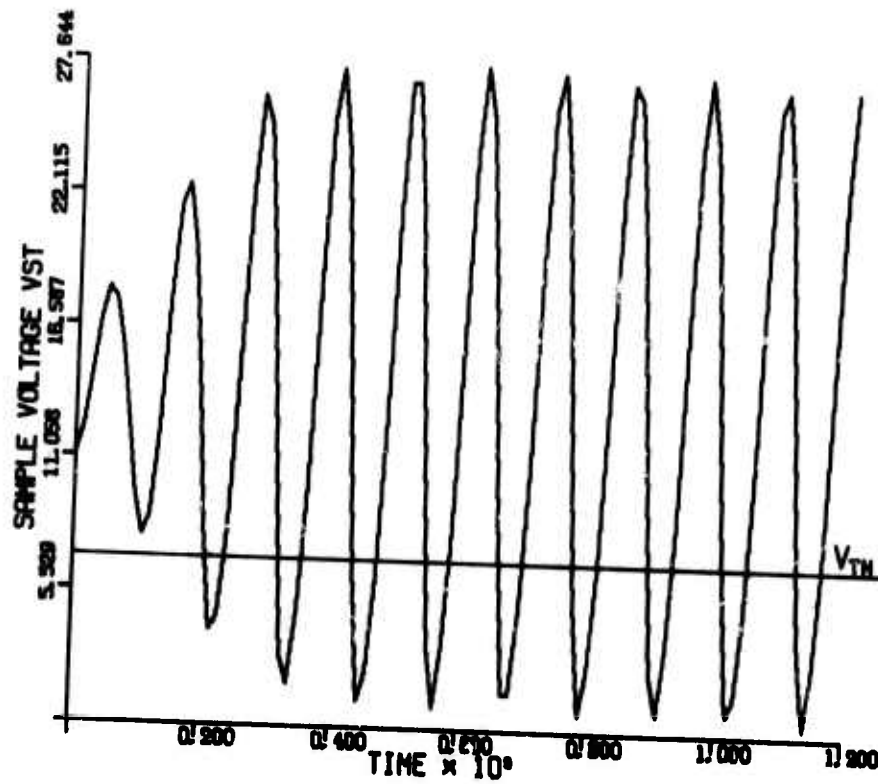


FIG. 12: V_{ST} vs. Time

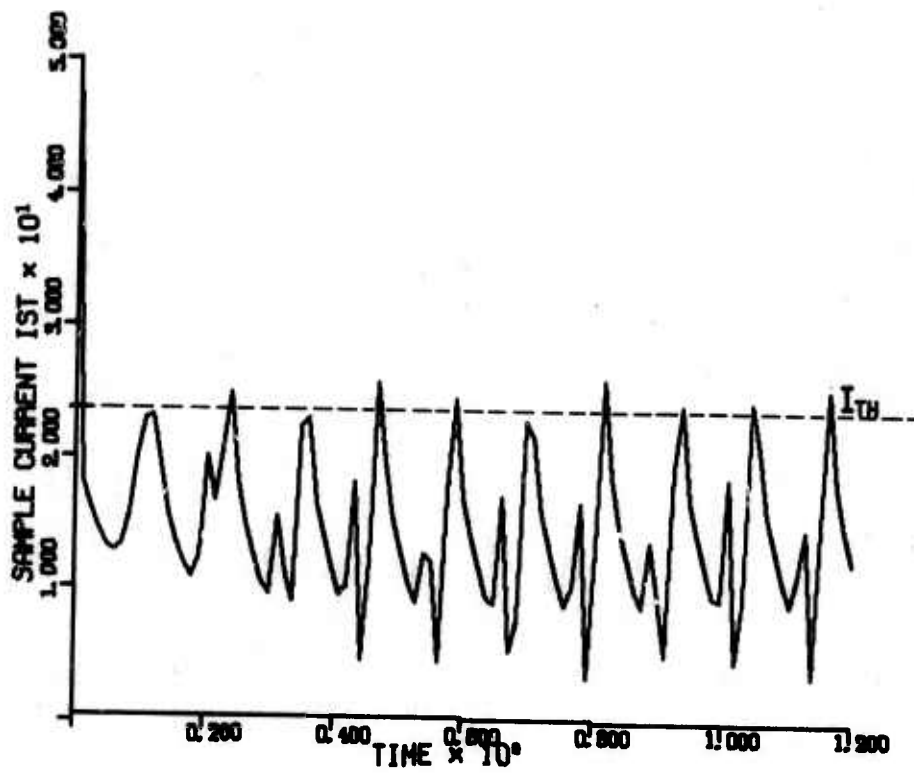


FIG. 13: I_{ST} vs. Time

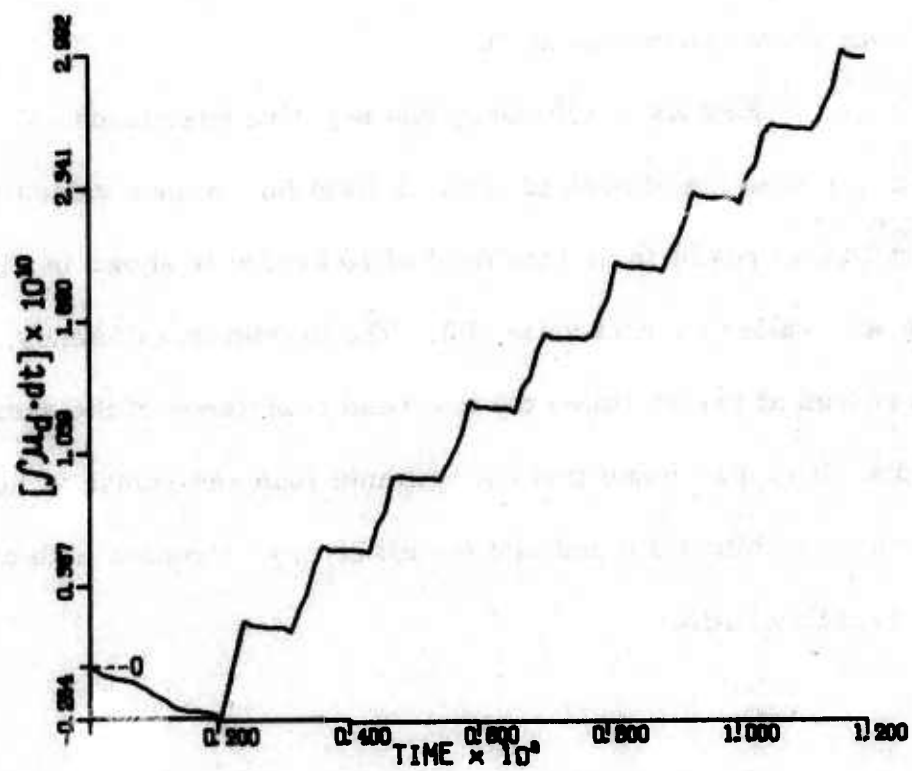


FIG. 14: Integral of Differential Mobility
W. R. T. Time vs. Time

cycle continually decreased with a corresponding increase in efficiency.

The slope finally became zero as the efficiency reached a maximum.

Thus, the optimum rf loading was that for which the net contribution to $\int u_d dt$ over an rf period was zero.

Results of efficiency and negative resistance have been obtained as a function of peak rf electric field for various values of bias field. A typical result for a bias field of 10 kv/cm is shown in Fig. 15 for a peak to valley current ratio of 2. The maximum efficiency, obtained with an rf load at twelve times the low-field resistance of the sample, is about 15%. It is also found that the optimum load resistance is larger for higher values of bias field and that the efficiency increases with an increase in peak to valley ratio.

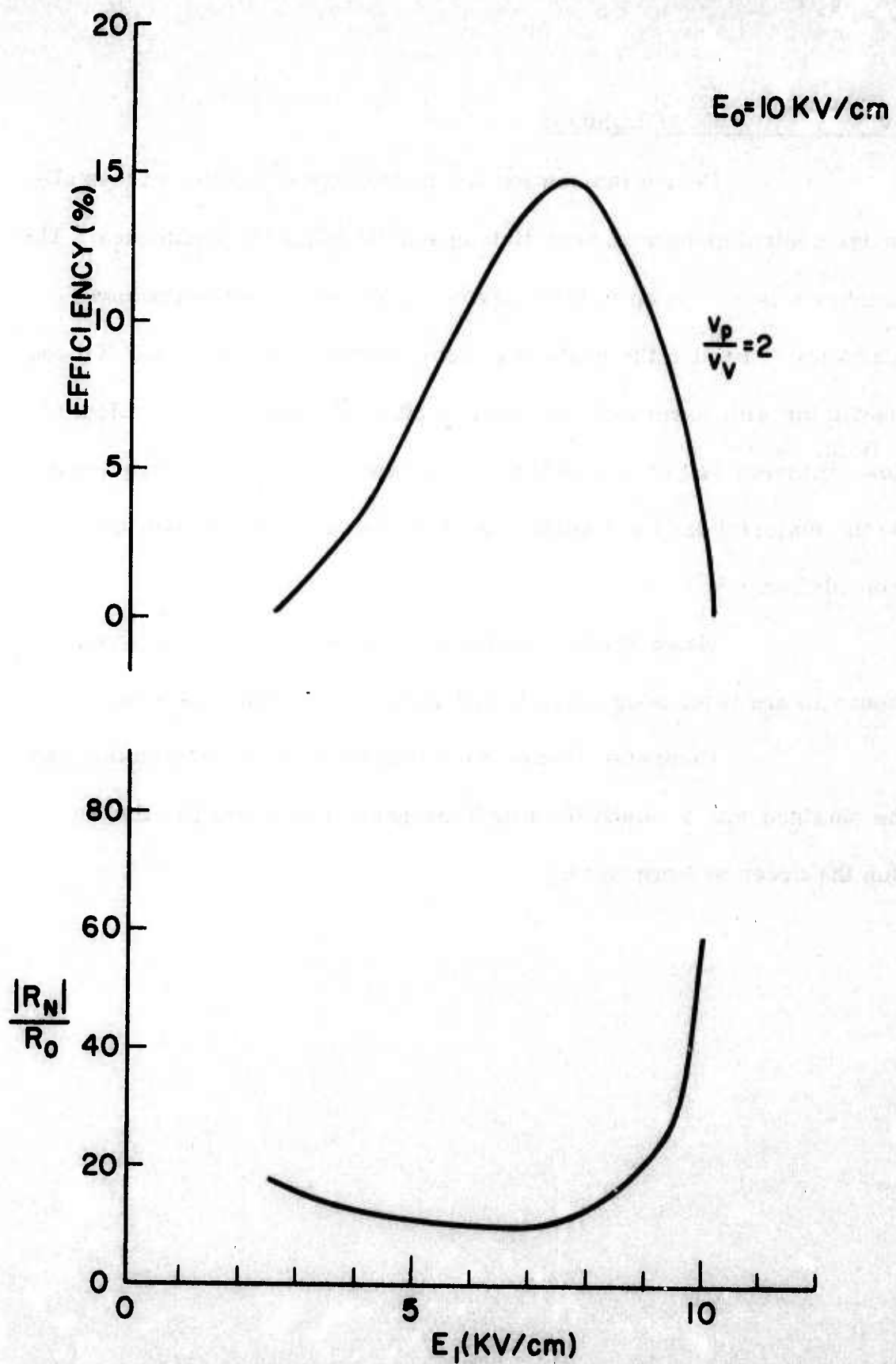


FIG. 15 Efficiency And Normalized Negative Resistance vs. RF Field for a Bias Field Of 10KV/CM

IV. CONCLUSIONS

Device fabrication and technology are quite successfully under control along with heat sinking and die attaching techniques. The emphasis is now on optimizing device parameters, and microwave circuitry to realize the goals of a highly stable, low noise, CW X-band oscillator with powers on the order of 30 to 100 MW. The problem of low efficiency ($\approx 1\%$) is tentatively being ascribed to doping gradients in the material used and initial experiments seem to bear out the correlation.

Noise studies are being made on a routine basis and controls are being sought which will allow further improvement.

Computer studies show that LSA design information can be obtained with a relatively simple program with short run times (on the order of 4 minutes).